Irrigation in JULES Land-Only Simulations over South and East Asia

Markus Todt[1,2], Pier Luigi Vidale[1,2], Patrick C. McGuire[1,2], Omar V. Müller[1,2,3]

[1]University of Reading, United Kingdom; [2]National Centre for Atmospheric Science, United Kingdom; [3]Universidad Nacional del Litoral, Argentina

This work and its contributors were supported by the UK-China Research & Innovation Partnership Fund through the Met Office Climate Science for Service Partnership (CSSP) China as part of the Newton Fund.

Background

Soil moisture controls heat and water fluxes from the land surface, which have a strong influence on regional weather and climate (*Betts, 2009*; *Seneviratne et al., 2010*). Soil moisture in turn responds to atmospheric forcing, providing a feedback mechanism in the coupled system. Capturing these feedbacks in a weather or climate model requires realistic simulation of various land surface processes, however, irrigation and other water management methods are still missing in most climate-modelling studies today.

Irrigation has been shown to alter turbulent heat fluxes, increasing evapotranspiration and reducing surface and air temperatures, and to subsequently affect regional weather and climate even masking the effects of global warming (*Bonfils and Lobell, 2007*; *Kueppers et al., 2007*; *Sacks et al., 2009*; *Qian et al., 2013*; *Kang and Eltahir, 2019*; *Thiery et al., 2020*). Comparison with observations has further demonstrated the impact of missing irrigation on surface fluxes during dry spells in climate models (*Gallego-Elvira et al., 2019*). Areas of particular interest are the Indo-Gangetic Plain and the North China Plain, as these regions are dominated by irrigated agriculture (*Siebert et al., 2015a*) and exhibit high sensitivity of surface fluxes to soil moisture in climate models (*Dirmeyer, 2011*; *Dirmeyer et al., 2014*). The role of irrigation is also of fundamental importance for studies of stress to ecosystems and human beings under climate change, which must include consideration of the combined effect of temperature and moisture (*Kang and Eltahir, 2018*; *Mishra et al., 2020*).

Irrigation parameterizations of varying complexity have recently been used in several global land and climate models (e.g. *Guimberteau et al., 2012*; *Pokhrel et al., 2017*; *Thiery et al., 2017*). An irrigation scheme is available optionally in the Joint UK Land Environment Simulator (JULES), land component of the Met Office Unified Model (MetUM), which prevents water stress in the top soil (*Harding et al., 2013*; *Gedney et al., 2014*; *Williams and Falloon, 2015*; *Williams et al., 2017*; *Franke et al., 2020*). However, the simulation of irrigation and its impact on surface fluxes in JULES has so far not been assessed on a spatial scale.

JULES & Irrigation

The Joint UK Land Environment Simulator (JULES) is a land surface model that both serves as the land component in the Met Office Unified Model and can be used as a standalone (land-only) model (*Best et al., 2011*; *Clark et al., 2011*). Heterogeneity of the land surface is represented in JULES through tiling of grid cells, which allows for the distinction of different vegetated surface types and four non-vegetated surface types (urban, inland water, soil, and land ice) assigning a fraction for each surface type (from 0 to 1) to each grid cell. State variables and surface fluxes are calculated separately for each surface type in a grid cell, while all surface types share a single soil column. Soil is subdivided into 4 layers in the default JULES setting with increasing layer thickness from top to bottom, covering 10cm, 25cm, 65cm, and 200cm, respectively. A parameterisation based on TOPMODEL (TOPography-based hydrological MODEL) is available optionally in JULES to represent the effect of sub-grid variability of soil moisture, which also introduces a groundwater storage with a thickness of 3m beneath the soil layers (*Best et al., 2011*; *Marthews et al., 2015*). When the TOPMODEL-based parameterisation is active, water can drain from the soil layers into the groundwater layer and water draining from the groundwater layer constitutes sub-surface runoff.

A simple representation of irrigation has been implemented in JULES that replenishes soil water in the top two soil layers to field capacity on a daily basis, so that vegetation does not experience water stress (*Gedney et al., 2014*; *Williams et al., 2017*). The TOPMODEL-based parameterization needs to be activated in order to physically limit the amount of irrigation, in which case irrigation water is taken firstly from the groundwater layer and secondly from river storage. Irrigation can be applied to each vegetated surface type in JULES and is prescribed as a fraction for each grid cell similar to fractional coverage of surface types. This irrigation fraction is applied to the soil column, which results in separate soil moisture values for the irrigated and non-irrigated fractions in each layer. There are 3 different versions of the irrigation scheme in JULES that differ in determining the timing of irrigation throughout the year. This study uses the simplest version of the irrigation scheme, which applies irrigation throughout the year unless soil is frozen and does not require specific representation of crops. This version is currently being implemented in the MetUM.

Simulations & Observations

In this study, we have run simulations of JULES over South and East Asia, where two global hotspots of irrigation are located. The extent of irrigation prescribed in simulations was derived from a dataset of historical irrigation area.

Our simulations retain the default, widely used land surface configuration of JULES, demonstrating the usage of irrigation in a way that is consistent with general climate-modelling studies using JULES. We created simulation ensembles by varying spin-up choices and irrigation extent.

Simulation of irrigation and its impact on turbulent fluxes was assessed by comparison with observational estimates. For this, we used reconstructions of irrigation from hydrological models and combined observational/machine-learning products for turbulent fluxes.

Back

Domain & Irrigation Extent

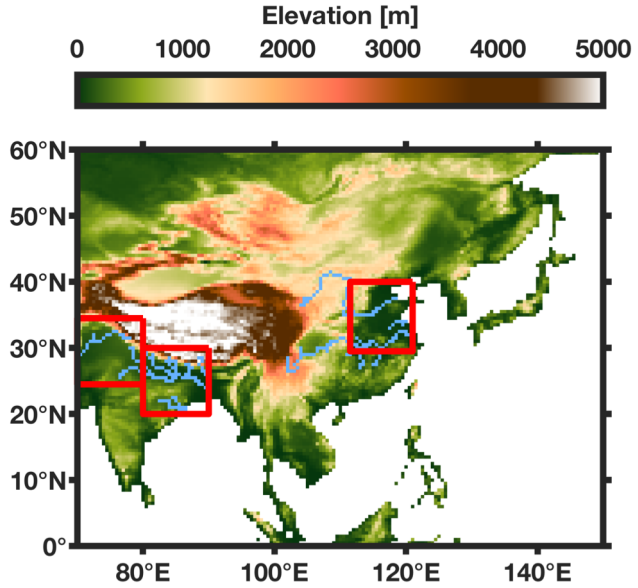

The focus of this study is South and East Asia, which features two global hotspots of irrigation in the Indo-Gangetic Plain and the North China Plain. Focus areas for this study are indicated by red rectangles: North China Plain and surroundings (**NCP**; containing rivers Huang He, Huai He, and Chang Jiang from North to South), North-East India (**NEI**; containing rivers Ganges and Mahanadi from North to South), and North-West India and Pakistan (**NWI**; including river Indus).

Spatially varying irrigation fraction has to be prescribed for JULES in order to represent the extent of irrigation across the simulation domain, which was derived from a dataset of historical area equipped for irrigation (AEI; *Siebert et al., 2015a,b*). This dataset covers the period 1900 to 2005, with AEI in 10-year increments before 1980 and 5-year increments afterwards. Several irrigation area products are available from the dataset, and AEI_HYDE_FINAL_IR was used in this study as it ”has maximum consistency with the sub-national irrigation statistics” (*Siebert et al., 2015a*).

Simulations run for this study represent land cover using the default setting of 5 vegetated surface types (broadleaf trees, evergreen trees, C3 grass, C4 grass, and shrubs) without a specific representation of crops. Instead, irrigation was applied to C3 grass, which was used as a proxy for crops, and irrigation fraction derived from AEI was limited to coverage by C3 grass for each grid cell.

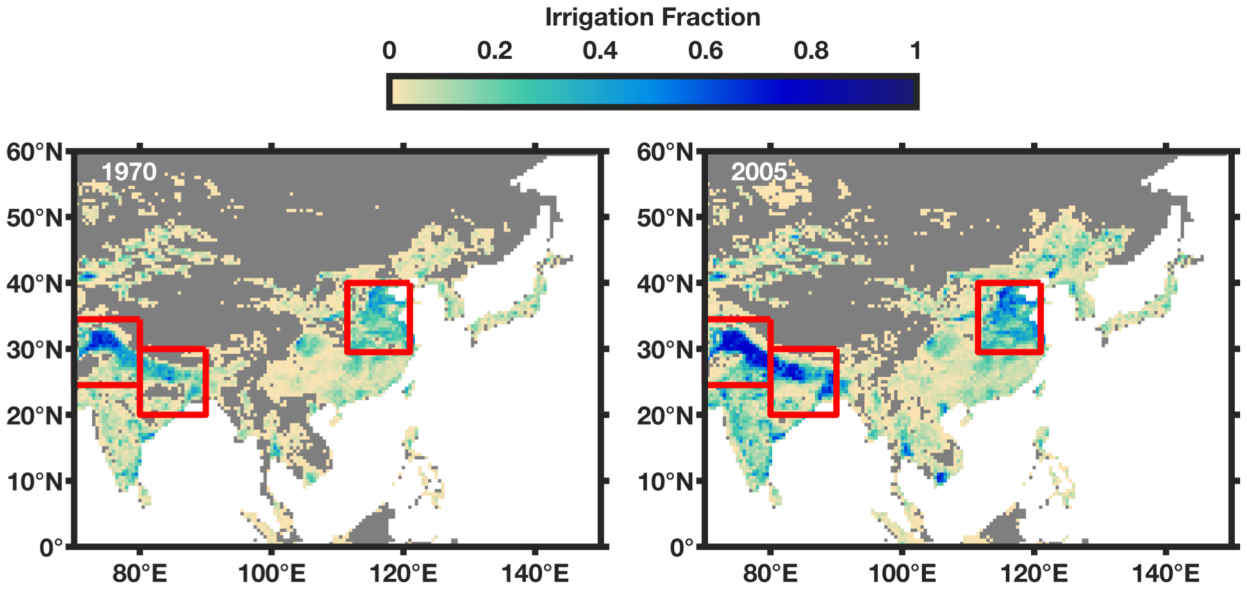

Simulations

Fractional coverage of surface tiles was prescribed based on International Geosphere–Biosphere Programme (IGBP) land classifications, with the original 17 land classes being aggregated to 9 tiles in JULES (*Walters et al., 2019*). Seasonal cycles of leaf area index (LAI) were prescribed for each vegetation tile in each grid cell based on Moderate Resolution Imaging Spectroradiometer (MODIS) observations of LAI, shown here as averages for C3 grass over focus areas. Vegetation height was derived from LAI and prescribed as temporally constant for each vegetation tile. The process of deriving LAI and canopy height is explained by *Wiltshire et al. (2020)*. Simulations were driven with 0.5º-resolution WFDEI (WATCH Forcing Data ERA-Interim) meteorological forcing data for 1979 to 2012 (*Weedon et al., 2018*).

Two sets of simulations were run for this study, one with TOPMODEL but without irrigation (henceforth, **CTRL**) and one with TOPMODEL and irrigation (henceforth, **IRRG**). Since the irrigation scheme draws from groundwater in this study, usage of irrigation during spin-up as well as spin-up duration modulate the availability of water for irrigation and thus its impact. We test the sensitivity of the impact of irrigation to spin-up choices by running spin-ups either with or without irrigation, by using either data for 1979 or data for 1979 to 1981, and by running spin-ups either for 33 years (11 cycles of 1979-1981 or 33 cycles of 1979) or for 99 years (33 cycles of 1979-1981 or 99 cycles of 1979). Irrigation fractions representing 1970 were prescribed for the spin-up periods, if used. After spin-up, irrigation fractions were prescribed as either representing 1970 or representing 2005. This results in an ensemble of 16 different simulations for IRRG (and 4 for CTRL): 2 (spin-ups over 1979 or 1979-1981) × 2 (spin-ups of 33 years or 99 years) × 2 (spin-ups with or without irrigation) × 2 (1970-level or 2005-level irrigation after spin-up). Simulations were analysed over the period 1982 to 2012 ignoring the years that were used for spin-up.

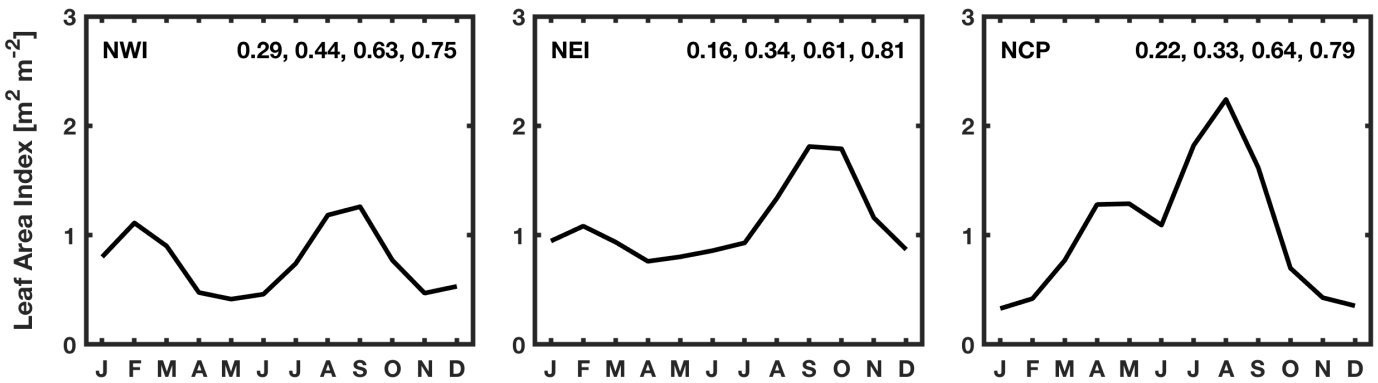

→ Numbers in the top right corner of each box indicate regional averages of irrigation fraction for 1970, irrigation fraction for 2005, coverage by C3 grass, and vegetation coverage (from left to right).

Back

Observations & Observational Estimates

Simulations are compared to products for latent heat fluxes and sensible heat fluxes from the FLUXCOM ensemble of global land-atmosphere energy fluxes (*Jung et al., 2019*), which are the successor dataset to global biosphere-atmosphere flux (GBAF) products that are used as references in the International Land Model Benchmarking System (ILAMB; *Collier et al., 2018*). The FLUXCOM observational estimates have been derived from FLUXNET energy flux measurements and remote sensing as well as meteorological data by training machine-learning algorithms (*Tramontana et al., 2016*; *Jung et al., 2019*). For this study, we used two FLUXCOM datasets, one that only incorporates remote-sensing data with FLUXNET observations (henceforth, **RS**), which covers 2001 to 2012, and one that incorporates remote-sensing data as well as WFDEI data with FLUXNET observations (henceforth, **RS+WFDEI**), which covers 1979 to 2012.

Simulated irrigation is compared to reconstructions of irrigation water consumption and water withdrawal for irrigation, which derived water consumption from water withdrawal through estimated water use efficiency (*Huang et al., 2018b*). These reconstructions were created by using 4 different hydrological models to temporally and spatially downscale country-scale estimates of water use yielding 4 estimates (*Huang et al., 2018a*). This product was chosen for comparison as the hydrological models were driven by WFDEI forcing data, the same as used for simulations in this study, and the same underlying water-use data were used to create the AEI product, from which irrigation fraction was derived for simulations in this study.

Impact on Surface Fluxes

Seasonal cycles of irrigation, soil moisture, and surface fluxes are shown for regional averages over focus areas North-West India and Pakistan (NWI), North-East India (NEI), and North China Plain and surroundings (NCP). Irrigation timing is similar across regions with a bimodal seasonal cycle, which features a peak in boreal spring (pre-monsoon season) and a smaller peak in boreal autumn (post-monsoon season). Irrigation is applied throughout the year over NWI and NCP, while there is no irrigation during the monsoon season over NEI. This is because there is little to no water stress to vegetation over NEI during the monsoon season as indicated by the soil moisture availability factor, which translates soil moisture into a fraction between wilting point (0) and no water stress (1). Irrigation generally increases soil moisture content (SMC) in the top soil layers, which increases soil water available to vegetation over NCP and NWI. Over NEI, water stress to vegetation is increased during the pre-monsoon dry season in IRRG despite increased SMC in the top soil layers, as total-column SMC is reduced in IRRG throughout the year (more under "Water Fluxes…").

Irrigation results in an increase in GPP over all focus areas, which is scaled by irrigation magnitude and corresponds to changes in water stress to vegetation. However, the impact of irrigation on GPP is limited in these simulations because vegetation is not modelled dynamically. Irrigation increases latent heat fluxes (LHF) and decreases sensible heat fluxes (SHF), and this effect is also scaled by irrigation magnitude. The impact of irrigation on the partitioning of turbulent fluxes is largest during boreal spring, when both irrigation magnitude and SHF peak. This shift from SHF to LHF is substantially smaller over NCP than over NWI and NEI and reaches up to 30 Wm^{-2} over NEI. There is little to no range in irrigation, and consequently in its impact on surface fluxes, within the simulation ensemble IRRG over NCP and NWI, indicating a constraint on water for irrigation.

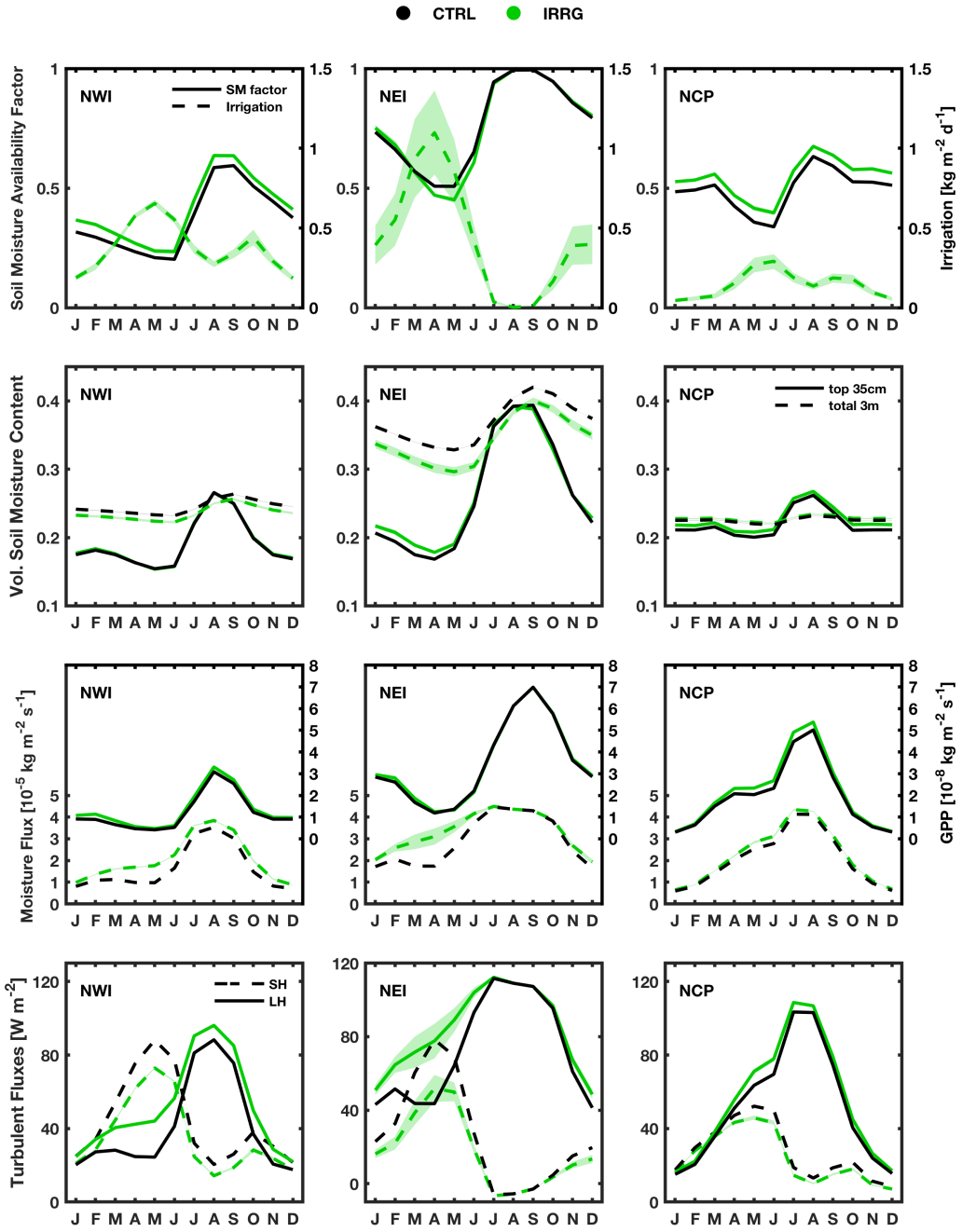

Home

Biases in Turbulent Fluxes

Simulations capture the seasonality of turbulent fluxes over focus areas when compared to FLUXCOM products (RS and RS+WFDEI), showing a peak in sensible heat fluxes (SHF) during the pre-monsoon dry season and a peak in latent heat fluxes (LHF) during the monsoon season. Simulations without irrigation underestimate LHF during the pre-monsoon season and SHF during the monsoon season across focus areas, with the low bias in SHF over North-East India (NEI) continuing after the monsoon season. The sum of turbulent fluxes is generally lower in simulations than in both FLUXCOM products, which contributes to underestimations of individual turbulent fluxes in JULES. **Irrigation increases LHF and decreases SHF, which reduces biases in LHF but exacerbates biases in SHF over the North China Plain (NCP) and North-West India & Pakistan (NWI).** Over North-East India, substantial irrigation during the pre-monsoon season results in a positive bias in LHF and a negative bias in SHF, so that LHF and SHF are overestimated and underestimated, respectively, throughout the year.

Maps show substantial negative biases in simulated LHF over the Indus Plain and North China Plain, which are reduced by irrigation. Irrigation increases LHF by 5-20 Wm^{-2} over the North China Plain, with highest increases along the Huang He river and during JJA. LHF is increased by up to 50 Wm^{-2} along the Indus river, but irrigation is only applied in parts of the region that shows a substantial negative bias in LHF. Irrigation increases LHF over the Ganges Plain by 20-50 Wm^{-2} during MAM, which turns biases from underestimation to overestimation and increases biases in absolute terms. Outside of MAM, irrigation slightly increases LHF over the Ganges Plain, increasing positive biases in JULES. **Although LHF simulated without the effect of irrigation displays substantial negative biases over regions where irrigation is applied, biases independent of irrigation dominate over South and East Asia.**

Despite regional averages indicating underestimated SHF, **bias maps show positive biases in SHF over core irrigation areas that are reduced by irrigation.** Substantial negative biases in SHF, which are independent of irrigation, contribute to the regional averages and are exacerbated where irrigation is applied. **As seen for LHF, the impact of irrigation over the Indus Plain and the North China Plain is mainly limited to river grid cells, and substantial irrigation over the Ganges Plain during JJA exacerbates biases.** Apart from the Indus Plain and the North China Plain, SHF is generally underestimated in JULES across South and East Asia outside of the pre-monsoon dry season.

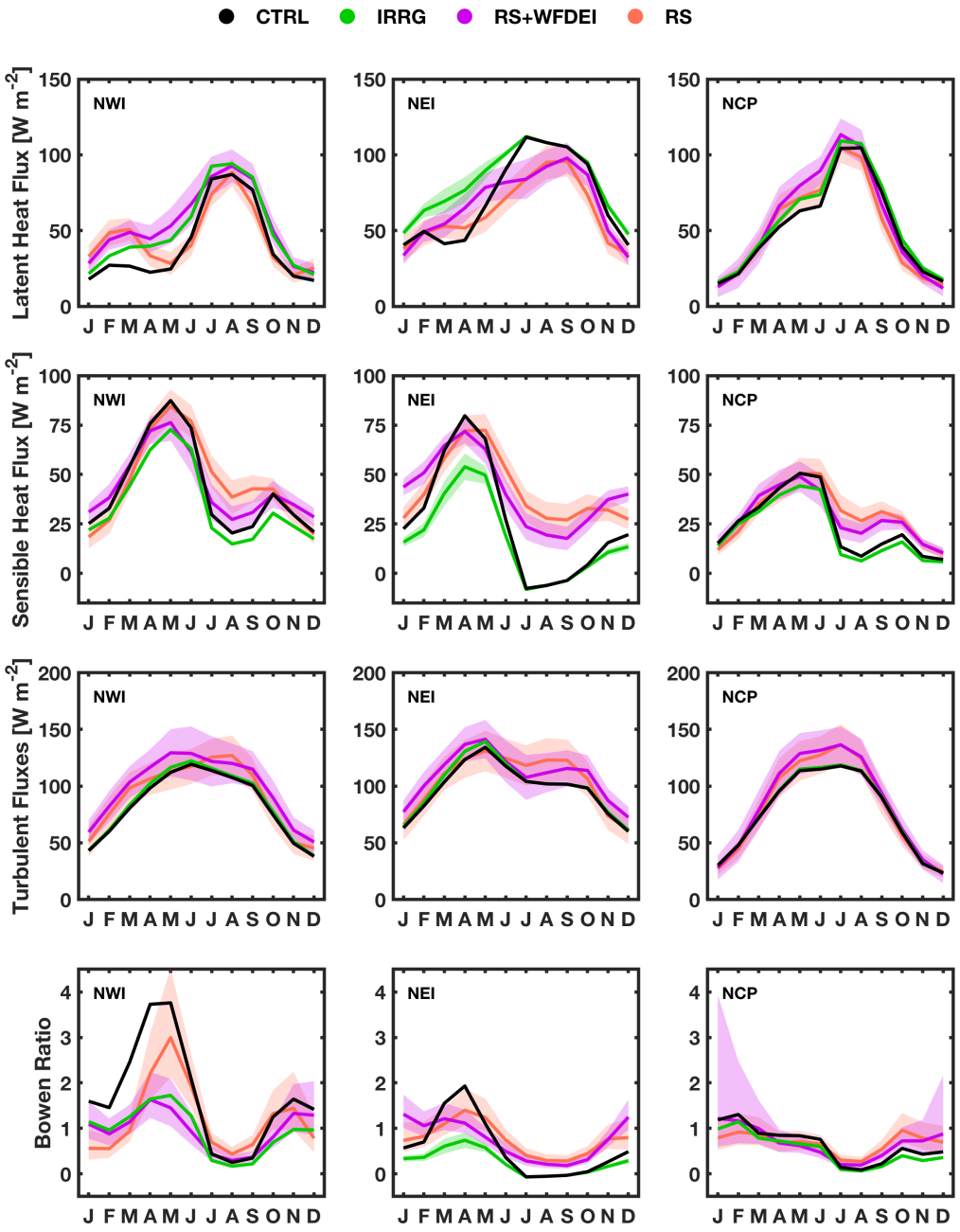

Back

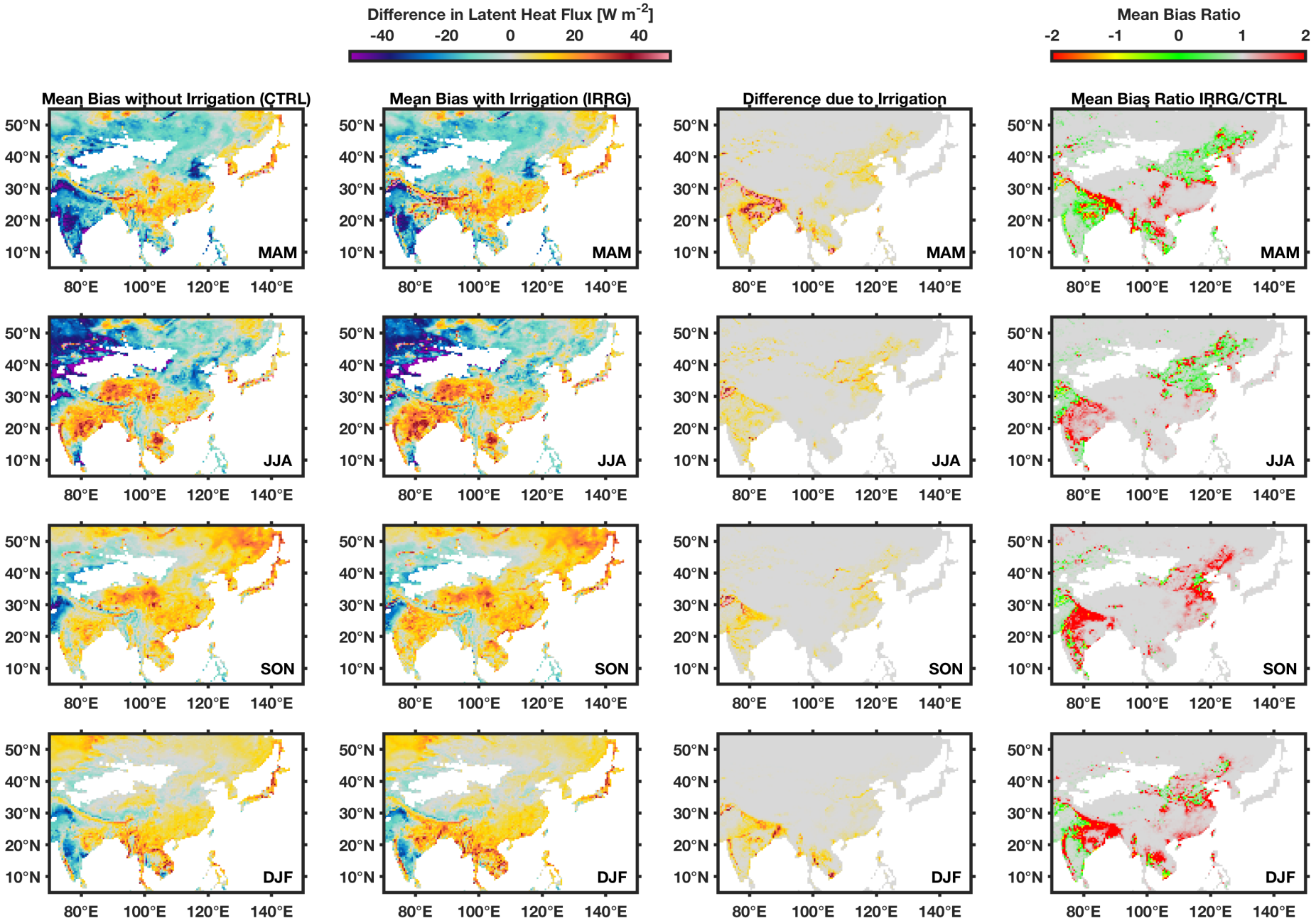

Bias maps are shown for one ensemble member relative to RS+WFDEI over 1982-2012. The particular ensemble member from IRRG was chosen as it includes irrigation during spin-up, i.e. prior to 1979, and 2005-level irrigation. Biases and bias ratios are only marginally different when the corresponding ensemble member without irrigation during spin-up is chosen. The ensemble member chosen for CTRL corresponds to the one for IRRG based on spin-up data and length.

Back

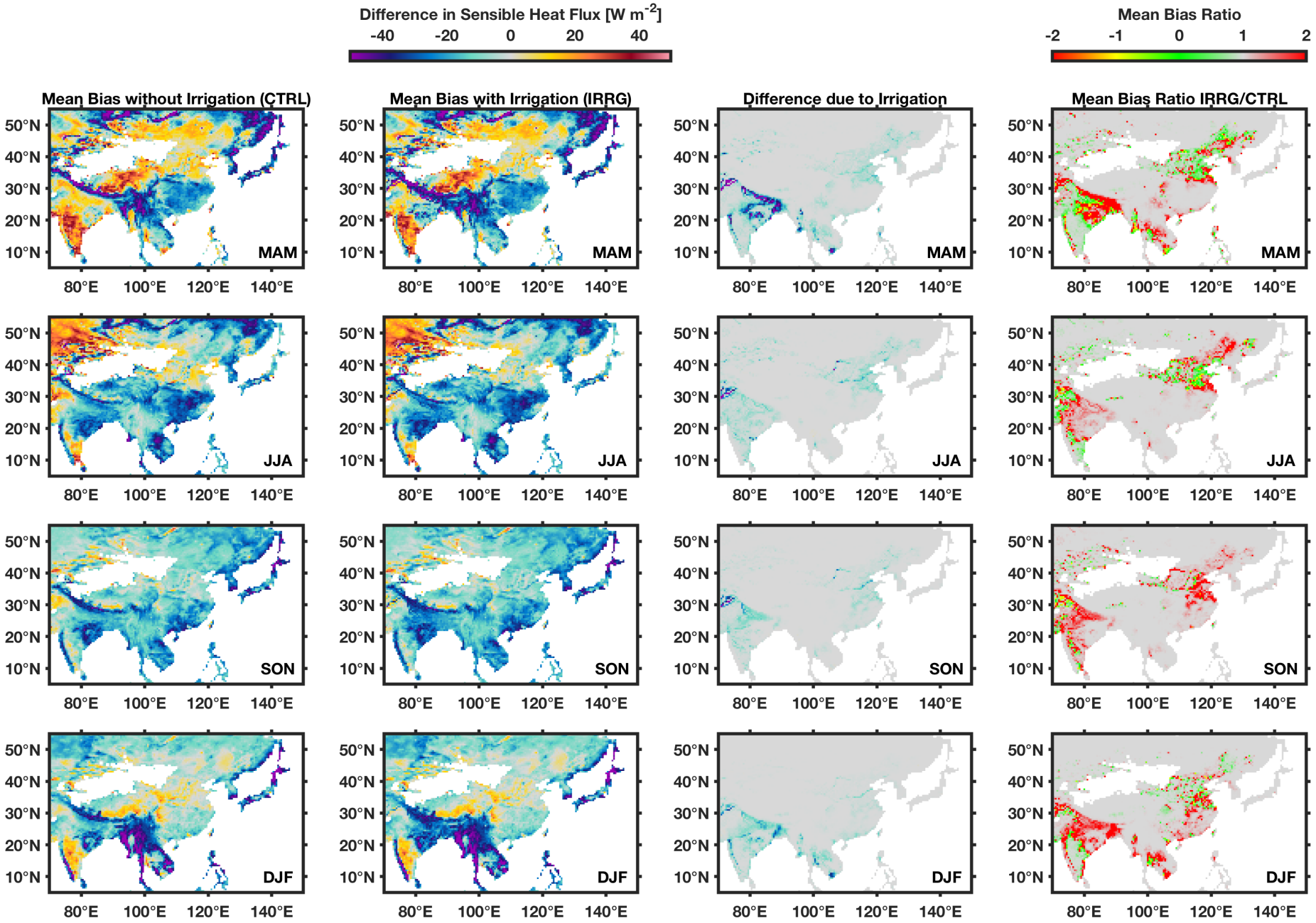

Bias maps are shown for one ensemble member relative to RS+WFDEI over 1982-2012. The particular ensemble member from IRRG was chosen as it includes irrigation during spin-up, i.e. prior to 1979, and 2005-level irrigation. Biases and bias ratios are only marginally different when the corresponding ensemble member without irrigation during spin-up is chosen. The ensemble member chosen for CTRL corresponds to the one for IRRG based on spin-up data and length.

Water Fluxes & Irrigation Sources

Irrigation also affects water fluxes throughout the soil column. Irrigation generally results in an increase in evapotranspiration of the same or similar magnitude. Over the North China Plain (NCP), there is little to no change from CTRL to IRRG in both runoff and drainage from soil layers into the groundwater layer. The lack of change in drainage despite extraction of water for irrigation indicates depletion of the groundwater layer. Irrigation leads to a reduction in river flow over NCP, which indicates extraction of water as runoff is unchanged. The small range in reduction of river flow across the ensemble suggests a quick depletion of the groundwater layer and that the contribution from rivers to irrigation is similar across simulations, i.e. independent of spin-up choices. Irrigation sources differ between North-East India (NEI) and North-West India & Pakistan (NWI). Over the Ganges Plain, water for irrigation mostly stems from groundwater, as irrigation leads to similar reductions in runoff and river flow over NEI. Extraction of groundwater over the Ganges Plain increases drainage from soil layers to the groundwater layer. This reduces runoff but not enough to balance the increase in drainage, which results in a reduction of SMC. Over NWI, which is comprised of the Indus Plain and the westernmost part of the Ganges Plain, reduction in river flow due to irrigation is substantially larger than reduction in runoff, which indicates that rivers are the main source for irrigation.

Contribution from rivers to irrigation in simulations is estimated in the table, separating simulations with and without irrigation during spin-up. Extraction of water from rivers generally increases over time, however, in contrast to NWI and NCP, the vast majority of water for irrigation over NEI is taken from the groundwater layer independent of simulation and period. **Irrigation depletes the groundwater layer over the Indus Plain and North China Plain in all simulations, independent of usage of irrigation during spin-up, so that rivers are the main source for irrigation by the end of the simulation period.**

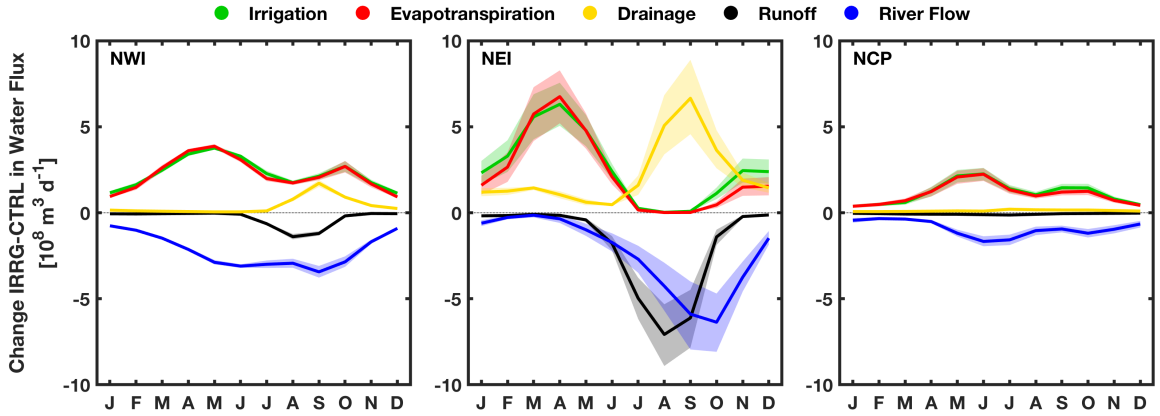

$$\left(\sum_{m=1}^{12} \Delta \text{ River Flow} - \sum_{m=1}^{12} \Delta \text{ Runoff} \right) / \sum_{m=1}^{12} \text{Irrigation}$$

Subset	NWI 1982-93	NWI 2001-12	NEI 1982-93	NEI 2001-12	NCP 1982-93	NCP 2001-12
IRRG w/o	79%	82%	15%	20%	42%	81%
IRRG w/	82%	82%	15%	20%	62%	84%

Comparison with Irrigation Estimates

Irrigation simulated by JULES is compared to reconstructions of water consumption and water withdrawal for irrigation. In these reconstructions, water consumption and water withdrawal are related through irrigation efficiency, with water withdrawal being roughly twice the amount of water consumption. There is no irrigation efficiency in JULES, as irrigation is directly applied to soil layers, so that irrigation in JULES corresponds to reconstructed water consumption regarding its impact on surface fluxes. **Simulated irrigation is similar to reconstructed water consumption over North-West India & Pakistan (NWI) and the North China Plain (NCP) outside of the monsoon season, during which simulated irrigation is lower than in the reconstruction.** In particular, simulated irrigation over NWI features two peaks, one before and one after the monsoon season, while reconstructed irrigation displays little change from June to October. Despite irrigation in JULES depleting the groundwater layer over NWI and NCP, water extracted for irrigation in IRRG is substantially less than reconstructed water withdrawal. **Over North-East India (NEI), simulated irrigation is substantially higher than reconstructed irrigation during the pre-monsoon season**, compared to both consumption and withdrawal. Overall, simulated irrigation is highest over NEI while reconstructed irrigation is lowest over NEI.

Maps of irrigation in simulations and reconstructed consumption further illustrate the dependence on river flow over NWI and NCP in simulations. While magnitudes of maximum irrigation are similar between simulations and reconstruction, simulated irrigation over NWI is limited to river grid cells and missing in between the Indus Plain and the Ganges Plain. Over NCP, irrigation in simulations is highest along the Huang He, which is not the case in reconstructions. Irrigation over North-East India before the monsoon season is substantially higher in IRRG than in the reconstruction, and there is irrigation in IRRG over Eastern India where the reconstruction shows little to no irrigation.

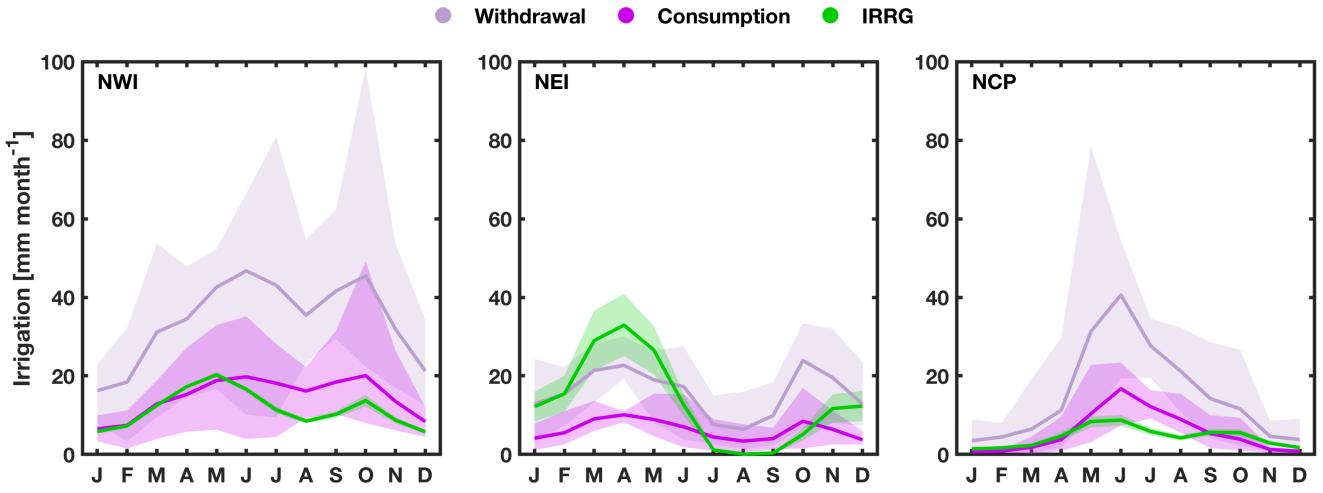

Back

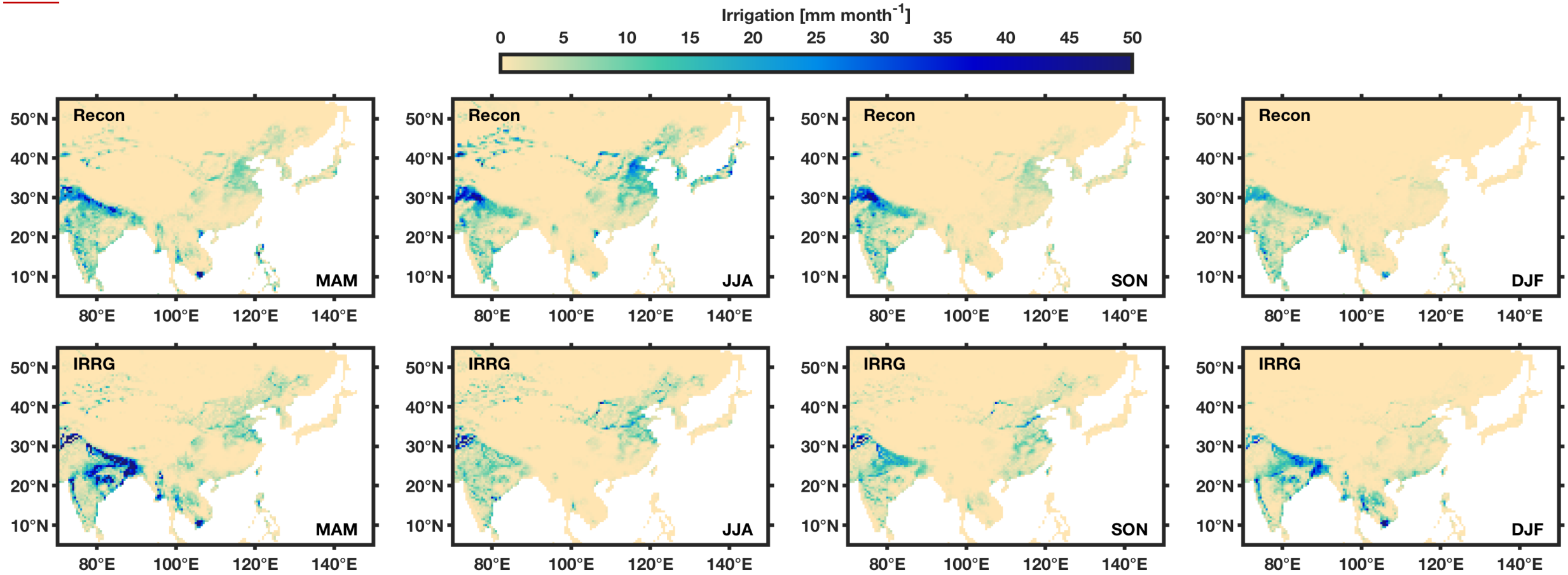

Maps show ensemble-mean reconstructed irrigation consumption (i.e. after application of efficiency) and irrigation for one ensemble member of IRRG. The particular ensemble member includes irrigation during spin-up, i.e. prior to 1979, and 2005-level irrigation, but maps are not substantially different when the ensemble member with irrigation fraction for 1970 and without irrigation during spin-up is shown.

Note that the ensemble member is the same as the one used for maps of biases in turbulent fluxes.

Conclusions

The irrigation scheme in JULES is generally able to capture the seasonality and magnitude of irrigation over the North China Plain and the Indus Plain but overestimates irrigation over the Ganges Plain compared with reconstructions of irrigation. Introduction of irrigation in JULES increases evapotranspiration and primary productivity, increases latent heat fluxes, and decreases sensible heat fluxes.

Comparison with combined observational/machine-learning products shows that irrigation improves the simulation of turbulent fluxes in JULES over the North China Plain and the Indus Plain but exacerbates biases over the Ganges Plain. However, biases in turbulent fluxes over South and East Asia unrelated to irrigation are larger than changes in turbulent fluxes due to irrigation.

Furthermore, the irrigation scheme rapidly depletes groundwater storage, suggesting the representation of groundwater in JULES restricts the amount of water available for irrigation and might be insufficient for the simulation of physically-constrained irrigation.

References

Best, M. J., Pryor, M., Clark, D. B., Rooney, G. G., Essery, R. L. H., Ménard, C. B., Edwards, J. M., Hendry, M. A., Porson, A., Gedney, N., Mercado, L. M., Sitch, S., Blyth, E., Boucher, O., Cox, P. M., Grimmond, C. S. B., and Harding, R. J.: The Joint UK Land Environment Simulator (JULES), model description – Part 1: Energy and water fluxes, Geoscientific Model Development, 4, 677–699, https://doi.org/10.5194/gmd-4-677-2011, https://www.geosci-model-dev.net/4/677/2011/, 2011.

Betts, A. K.: Land-Surface-Atmosphere Coupling in Observations and Models, Journal of Advances in Modeling Earth Systems, 1, https://doi.org/10.3894/JAMES.2009.1.4, https://agupubs.onlinelibrary.wiley.com/doi/abs/10.3894/JAMES.2009.1.4, 2009.

Bonfils, C. and Lobell, D.: Empirical evidence for a recent slowdown in irrigation-induced cooling, Proceedings of the National Academy of Sciences, 104, 13 582–13 587, https://doi.org/10.1073/pnas.0700144104, 2007.

Clark, D. B., Mercado, L. M., Sitch, S., Jones, C. D., Gedney, N., Best, M. J., Pryor, M., Rooney, G. G., Essery, R. L. H., Blyth, E., Boucher, O., Harding, R. J., Huntingford, C., and Cox, P. M.: The Joint UK Land Environment Simulator (JULES), model description – Part 2: Carbon fluxes and vegetation dynamics, Geoscientific Model Development, 4, 701–722, https://doi.org/10.5194/gmd-4-701-2011, 2011.

Collier, N., Hoffman, F. M., Lawrence, D. M., Keppel-Aleks, G., Koven, C. D., Riley,W. J., Mu, M., and Randerson, J. T.: The International Land Model Benchmarking (ILAMB) System: Design, Theory, and Implementation, Journal of Advances in Modeling Earth Systems, 10, 2731–2754, https://doi.org/10.1029/2018MS001354, 2018.

Dirmeyer, P. A.: The terrestrial segment of soil moisture–climate coupling, Geophysical Research Letters, 38, https://doi.org/10.1029/2011GL048268, 2011.

Dirmeyer, P. A., Wang, Z., Mbuh, M. J., and Norton, H. E.: Intensified land surface control on boundary layer growth in a changing climate, Geophysical Research Letters, 41, 1290–1294, https://doi.org/10.1002/2013GL058826, 2014.

Franke, J. A., Müller, C., Elliott, J., Ruane, A. C., Jägermeyr, J., Balkovic, J., Ciais, P., Dury, M., Falloon, P. D., Folberth, C., François, L., Hank, T., Hoffmann, M., Izaurralde, R. C., Jacquemin, I., Jones, C., Khabarov, N., Koch, M., Li, M., Liu, W., Olin, S., Phillips, M., Pugh, T. A. M., Reddy, A., Wang, X., Williams, K., Zabel, F., and Moyer, E. J.: The GGCMI Phase 2 experiment: global gridded crop model simulations under uniform changes in CO2, temperature, water, and nitrogen levels (protocol version 1.0), Geoscientific Model Development, 13, 2315–2336, https://doi.org/10.5194/gmd-13-2315-2020, 2020.

Gallego-Elvira, B., Taylor, C. M., Harris, P. P., and Ghent, D.: Evaluation of Regional-Scale Soil Moisture-Surface Flux Dynamics in Earth System Models Based on Satellite Observations of Land Surface Temperature, Geophysical Research Letters, 46, 5480–5488, https://doi.org/10.1029/2019GL082962, https://agupubs.onlinelibrary.wiley.com/doi/abs/10.1029/2019GL082962, 2019.

Gedney, N., Huntingford, C., Weedon, G. P., Bellouin, N., Boucher, O., and Cox, P. M.: Detection of solar dimming and brightening effects on Northern Hemisphere river flow, Nature Geoscience, 7, 796–800, https://doi.org/10.1038/ngeo2263, 2014.

Guimberteau, M., Laval, K., Perrier, A., and Polcher, J.: Global effect of irrigation and its impact on the onset of the Indian summer monsoon, Climate Dynamics, 39, 1329–1348, https://doi.org/10.1007/s00382-011-1252-5, 2012.

References

Harding, R., Blyth, E., Tuinenburg, O., and Wiltshire, A.: Land atmosphere feedbacks and their role in the water resources of the Ganges basin, Science of The Total Environment, 468-469, S85–S92, https://doi.org/10.1016/j.scitotenv.2013.03.016, 2013.

Huang, Z., Hejazi, M., Li, X., Tang, Q., Vernon, C., Leng, G., Liu, Y., Döll, P., Eisner, S., Gerten, D., Hanasaki, N., and Wada, Y.: Reconstruction of global gridded monthly sectoral water withdrawals for 1971–2010 and analysis of their spatiotemporal patterns, Hydrology and Earth System Sciences, 22, 2117–2133, https://doi.org/10.5194/hess-22-2117-2018, 2018a.

Huang, Z., Hejazi, M., Li, X., Tang, Q., Vernon, C., Leng, G., Liu, Y., Döll, P., Eisner, S., Gerten, D., Hanasaki, N., and Wada, Y.: Global gridded monthly sectoral water use dataset for 1971-2010: v2 (Version V2.0), https://doi.org/10.5281/zenodo.1209296, last access: 24th November 2020, 2018b.

Jung, M., Koirala, S., Weber, U., Ichii, K., Gans, F., Camps-Valls, G., Papale, D., Schwalm, C., Tramontana, G., and Reichstein, M.: The FLUXCOM ensemble of global land-atmosphere energy fluxes, Scientific Data, 6, 74, https://doi.org/10.1038/s41597-019-0076-8, 2019.

Kang, S. and Eltahir, E. A. B.: North China Plain threatened by deadly heatwaves due to climate change and irrigation, Nature Communications, 9, https://doi.org/10.1038/s41467-018-05252-y, 2018.

Kang, S. and Eltahir, E. A. B.: Impact of Irrigation on Regional Climate Over Eastern China, Geophysical Research Letters, 46, 5499–5505, https://doi.org/10.1029/2019GL082396, 2019.

Kueppers, L. M., Snyder, M. A., and Sloan, L. C.: Irrigation cooling effect: Regional climate forcing by land-use change, Geophysical Research Letters, 34, https://doi.org/10.1029/2006GL028679, 2007.

Marthews, T. R., Dadson, S. J., Lehner, B., Abele, S., and Gedney, N.: High-resolution global topographic index values for use in large-scale hydrological modelling, Hydrology and Earth System Sciences, 19, 91–104, https://doi.org/10.5194/hess-19-91-2015, 2015.

Mishra, V., Ambika, A. K., Asoka, A., Aadhar, S., Buzan, J., Kumar, R., and Huber, M.: Moist heat stress extremes in India enhanced by irrigation, Nature Geoscience, 13, 722–728, https://doi.org/10.1038/s41561-020-00650-8, 2020.

Pokhrel, Y. N., Felfelani, F., Shin, S., Yamada, T. J., and Satoh, Y.: Modeling large-scale human alteration of land surface hydrology and climate, Geoscience Letters, 4, 10, https://doi.org/10.1186/s40562-017-0076-5, 2017.

Qian, Y., Huang, M., Yang, B., and Berg, L. K.: A modeling study of irrigation effects on surface fluxes and land-air-cloud interactions in the southern great plains, Journal of Hydrometeorology, 14, 700–721, https://doi.org/10.1175/JHM-D-12-0134.1, 2013.

Sacks, W. J., Cook, B. I., Buenning, N., Levis, S., and Helkowski, J. H.: Effects of global irrigation on the near-surface climate, Climate Dynamics, 33, 159–175, https://doi.org/10.1007/s00382-008-0445-z, 2009.

References

Seneviratne, S. I., Corti, T., Davin, E. L., Hirschi, M., Jaeger, E. B., Lehner, I., Orlowsky, B., and Teuling, A. J.: Investigating soil moisture-climate interactions in a changing climate: A review, Earth-Science Reviews, 99, 125–161, https://doi.org/10.1016/j.earscirev.2010.02.004, 2010.

Siebert, S., Kummu, M., Porkka, M., Döll, P., Ramankutty, N., and Scanlon, B. R.: A global data set of the extent of irrigated land from 1900 to 2005, Hydrology and Earth System Sciences, 19, 1521–1545, https://doi.org/10.5194/hess-19-1521-2015, 2015a.

Siebert, S., Kummu, M., Porkka, M., Döll, P., Ramankutty, N., and Scanlon, B. R.: Historical Irrigation Dataset (HID), https://doi.org/10.13019/M20599, https://mygeohub.org/publications/8/2, 2015b.

Thiery, W., Davin, E. L., Lawrence, D. M., Hirsch, A. L., Hauser, M., and Seneviratne, S. I.: Present-day irrigation mitigates heat extremes, Journal of Geophysical Research: Atmospheres, 122, 1403–1422, https://doi.org/10.1002/2016JD025740, 2017.

Thiery, W., Visser, A. J., Fischer, E. M., Hauser, M., Hirsch, A. L., Lawrence, D. M., Lejeune, Q., Davin, E. L., and Seneviratne, S. I.: Warming of hot extremes alleviated by expanding irrigation, Nature Communications, 11, 290, https://doi.org/10.1038/s41467-019-14075-4, 2020.

Tramontana, G., Jung, M., Schwalm, C. R., Ichii, K., Camps-Valls, G., Ráduly, B., Reichstein, M., Arain, M. A., Cescatti, A., Kiely, G., Merbold, L., Serrano-Ortiz, P., Sickert, S., Wolf, S., and Papale, D.: Predicting carbon dioxide and energy fluxes across global FLUXNET sites with regression algorithms, Biogeosciences, 13, 4291–4313, https://doi.org/10.5194/bg-13-4291-2016, 2016.

Walters, D., Baran, A. J., Boutle, I., Brooks, M., Earnshaw, P., Edwards, J., Furtado, K., Hill, P., Lock, A., Manners, J., Morcrette, C., Mulcahy, J., Sanchez, C., Smith, C., Stratton, R., Tennant, W., Tomassini, L., Van Weverberg, K., Vosper, S., Willett, M., Browse, J., Bushell, A., Carslaw, K., Dalvi, M., Essery, R., Gedney, N., Hardiman, S., Johnson, B., Johnson, C., Jones, A., Jones, C., Mann, G., Milton, S., Rumbold, H., Sellar, A., Ujiie, M., Whitall, M., Williams, K., and Zerroukat, M.: The Met Office Unified Model Global Atmosphere 7.0/7.1 and JULES Global Land 7.0 configurations, Geoscientific Model Development, 12, 1909–1963, https://doi.org/10.5194/gmd-12-1909-2019, 2019.

Williams, K. E. and Falloon, P. D.: Sources of interannual yield variability in JULES-crop and implications for forcing with seasonal weather forecasts, Geoscientific Model Development, 8, 3987–3997, https://doi.org/10.5194/gmd-8-3987-2015, 2015.

Williams, K., Gornall, J., Harper, A., Wiltshire, A., Hemming, D., Quaife, T., Arkebauer, T., and Scoby, D.: Evaluation of JULES-crop performance against site observations of irrigated maize from Mead, Nebraska, Geoscientific Model Development, 10, 1291–1320, https://doi.org/10.5194/gmd-10-1291-2017, 2017.

Wiltshire, A. J., Duran Rojas, M. C., Edwards, J. M., Gedney, N., Harper, A. B., Hartley, A. J., Hendry, M. A., Robertson, E., and Smout-Day, K.: JULES-GL7: the Global Land configuration of the Joint UK Land Environment Simulator version 7.0 and 7.2, Geoscientific Model Development, 13, 483–505, https://doi.org/10.5194/gmd-13-483-2020, 2020.